Turbulence and Suspended Sediment Measurements in an Urban Environment during the Brisbane River Flood of January 2011

Richard Brown[1] and Hubert Chanson[2]

Abstract: In urbanized areas, flood flows constitute a hazard to populations and infrastructure, as illustrated during major floods in 2011. During the 2011 Brisbane River flood, some turbulent velocity data were collected using acoustic Doppler velocimetry in an inundated street. The field deployment showed some unusual features of flood flow in the urban environment. That is, the water elevations and velocities fluctuated with distinctive periods between 50 and 100 s linked with some local topographic effects. The instantaneous velocity data were analyzed using a triple decomposition. The velocity fluctuations included a large energy component in the slow fluctuation range, whereas the turbulent motion components were much smaller. The suspended sediment data showed some significant longitudinal flux. Altogether, the results highlighted that the triple decomposition approach originally developed for periodic flows is well-suited to complicated flows in an inundated urban environment. **DOI: 10.1061/(ASCE)HY.1943-7900.0000666.**

CE Database subject headings: Flood plains; Urban areas; Turbulence; Measurement; Suspended sediment; Rivers and streams; Australia.

Author keywords: Flood plain; Urban environment; Turbulence measurements; Triple decomposition; Suspended sediment concentration SSC; Water body resonance; Brisbane River.

Introduction

Flood flows in urbanized areas constitute a hazard to populations and infrastructure. Some recent catastrophes include the inundations of Vaison-la-Romaine (France) in 1992 and Nîmes (France) in 1998, the flooding of New Orleans (USA) in 2005, the floods in Queensland (Australia) in the summer of 2010–2011, and the Mississippi River flood (USA) in the spring of 2011. Flood flows in urban environments have only been studied relatively recently despite many centuries of flood events. Some researchers mentioned the storage effect in urban areas (Solo-Gabriele and Perkins 1997; Velickovic et al. 2011). Other studies looked into the flow patterns and redistribution in streets during storm events and the implication for flood modeling (Bates et al. 2004; Nania et al. 2004; Werner et al. 2005; Velickovic et al. 2011). A number of studies looked at the effect of floods on structures and buildings (Thieken et al. 2005). Some considered the potential impact of flowing waters on pedestrians (Asai et al. 2010; Ishigaki et al. 2003). However, to date, there are limited field observations and no basic methodology to analyze turbulent velocity measurements collected in a complex urban environment.

In this study, some turbulent velocity and suspended sediment concentration measurements were collected at relatively high frequency (50 Hz) in a flooded street during the January 12–13, 2011, flood of the Brisbane River (Australia) (Figs. 1 and 2). The results highlighted some difficulties in interpreting the raw data without proper decomposition. It is the aim of this work to present an innovative characterization of turbulence and sediment flux for an inundated urban environment. The field investigation and instrumentation are described in the next section. The primary results are presented in the following sections. The study is a detailed analysis of point measurements in an inundated urban setting rather than a detailed study of the whole flood event.

Field Investigation and Instrumentation

Investigation Site

Located along the Brisbane River, the central business district (CBD) of the city of Brisbane is approximately 25 km upstream of the river mouth [Fig. 1(a)], and the catchment area is 13,500 km^2 (Institution of Engineers, Australia 1974). Following some heavy rainfall in the catchment during early January 2011, the Brisbane River water level rose rapidly on January 11–12, 2011 (Chanson 2011). The city of Brisbane was flooded on January 11–14, with the flood waters peaking in the city early morning on January 13, 2011 [note that times throughout this paper are expressed in local Queensland time (GMT + 10)]. Fig. 3(a) shows the flood hydrograph of the Brisbane River at the City Gauge [location shown in Fig. 1(a)]. The data are compared with the predicted tidal level at the same location; both data and predictions were measured above the Australian height datum (AHD) (or mean sea level). At the peak of the flood, the estimated river discharge in the city reach was in excess of 9,000–10,000 m^3/s (T. Malone, personal communication, 2011), and the local friction slope was approximately 1×10^{-4} (Brown et al. 2011). The hydrograph data of the Brisbane River in the city (Fig. 3) may be compared to the peak levels of 5.45 m AHD in 1974 and 8.35 m AHD in 1893, while the

[1]Associate Professor, Queensland Univ. of Technology, Faculty of Built Environment and Engineering, Brisbane QLD 4000, Australia.

[2]Professor in Hydraulic Engineering, The Univ. of Queensland, School of Civil Engineering, Brisbane QLD 4072, Australia (corresponding author). E-mail: h.chanson@uq.edu.au

Note. This manuscript was submitted on October 21, 2011; approved on July 26, 2012; published online on August 7, 2012. Discussion period open until July 1, 2013; separate discussions must be submitted for individual papers. This paper is part of the ***Journal of Hydraulic Engineering***, Vol. 139, No. 2, February 1, 2013. © ASCE, ISSN 0733-9429/2013/2-244-253/$25.00.

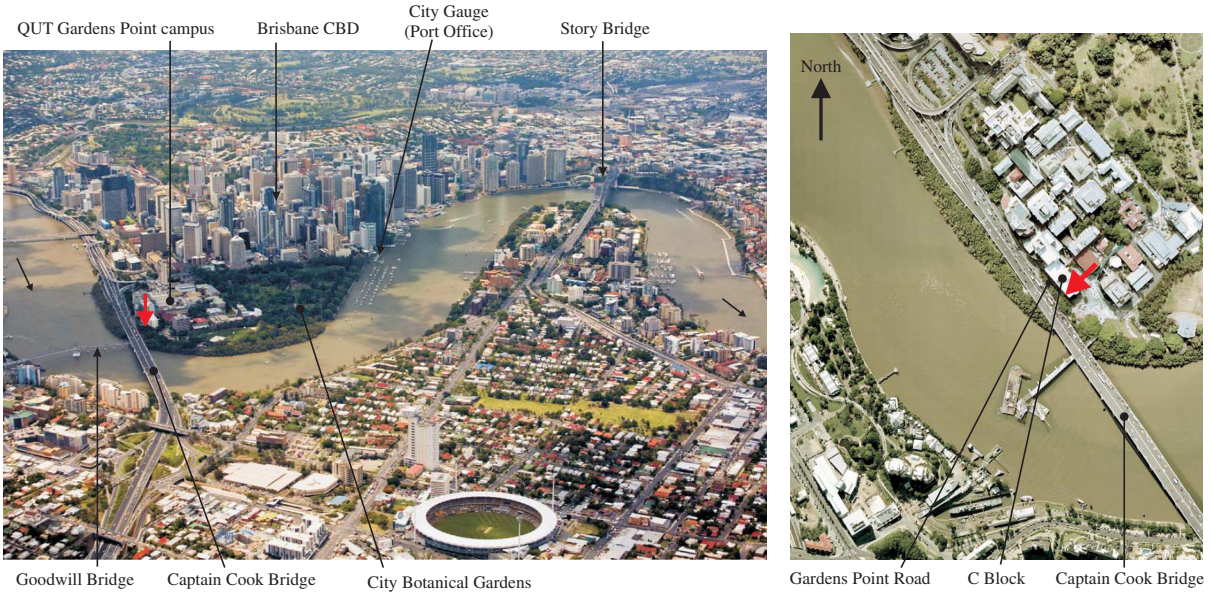

Fig. 1. Investigation site before flood: (a) aerial view of Brisbane's central business district in 2007 looking north (Copyright the University of Queensland)—Brisbane River flows from left to right—ADV sampling site is highlighted by arrow; (b) aerial view of Gardens Point Road and C Block building in 2001 (Copyright Queensland University of Technology)—ADV sampling site is highlighted by arrow

city experienced six major floods with higher water levels in the last 180 years (Chanson 2011).

Turbulent velocity measurements were performed along Gardens Point Road in the Queensland University of Technology (QUT) Gardens Point campus below the C Block building on January 12–14, 2011. The site was located between Gardens Point Road and the ground floor car park (Figs. 1 and 2). Fig. 1 shows some aerial views before the flood, with the thick arrow pointing to the sampling site. Fig. 2(a) presents a photograph taken during the flood and shows the acoustic Doppler velocimeter (ADV) locations. Fig. 2(b) details the ground floor car park of C Block building, and Fig. 2(c) shows a cross-sectional survey looking downstream. Further details, and photographs were reported by Brown et al. (2011).

Instrumentation

Free surface elevations were manually recorded using a measuring tape with reference to landmarks that were surveyed after the flood. The turbulent velocities were measured with a Sontek microADV (16 MHz, serial A843F) equipped with a three-dimensional (3D) side-looking head. For a series of data (Table 1, Series 1), the unit was placed horizontally with the head pointing downwards. After the ADV was dislodged by a timber log, the unit was repositioned vertically and attached to a hand rail (Location B, Series 2 and 3). During each series, the ADV was sampled continuously at 50 Hz (Table 1, third column). The ADV unit was equipped with a pressure sensor that was underwater and gave some instantaneous water elevation data during the first series of data (Series 1). During the other series, the pressure sensor was out of the water.

All the ADV data underwent a thorough postprocessing procedure to eliminate any erroneous or corrupted data from the data sets to be analyzed. The post processing included the removal of communication errors, the removal of average signal to noise ratio (SNR) data less than 5 dB, and the removal of average correlation values less than 60% (McLelland and Nicholas 2000). In addition, the phase-space thresholding technique developed by Goring and Nikora (2002) and extended by Wahl (2003) was applied to remove spurious points.

Sediment material was collected January 13–14, 2011, along Gardens Point Road. The soil samples consisted of fine mud ($d_{50} \approx 26$ μm). The calibration of the ADV unit in terms of suspended sediment concentration (SSC) was accomplished by measuring the signal amplitude of known, artificially produced concentrations of material obtained from the bed material sample, diluted in tap water, and thoroughly mixed. All the experiments were conducted on January 18, 2011, with the same microADV (serial A843F) using the same settings as for the field observations taken on January 12–14, 2011. The results indicated a decreasing signal amplitude with increasing SSC, linked with some signal attenuation previously observed in cohesive materials at high concentrations (Fig. 4) (Ha et al. 2009; Chanson et al. 2011).

Remarks

Two ADV settings were used (Table 1, fourth column). The lower velocity range was selected for the last two samplings after the flood started to recede, and slower velocities were observed.

During the field deployment, a number of problems were experienced. During the first series, the ADV was dislodged by the impact of a timber log and "wheelie" bin. The ADV unit was repositioned to a nearby handrail. During the second series, the ADV unit had to be stopped because the generator was required to assist flood victims whose homes were without electricity. A smaller generator was installed and the ADV was restarted two hours later. The third series ended when flood waters receded, and the upper ADV receiver came to be out of the water.

Basic Observations

During the rising stage of the Brisbane River flood January 11–12, the river swelled and inundated Gardens Point Road (Fig. 2). The left flood plain included some car parks located beneath Captain Cook Bridge [Fig. 2(a)], Gardens Point Road, and beneath a number of buildings [Fig. 2(c)]. Although a relatively fast flow motion was observed along Gardens Point Road, visual and photographic

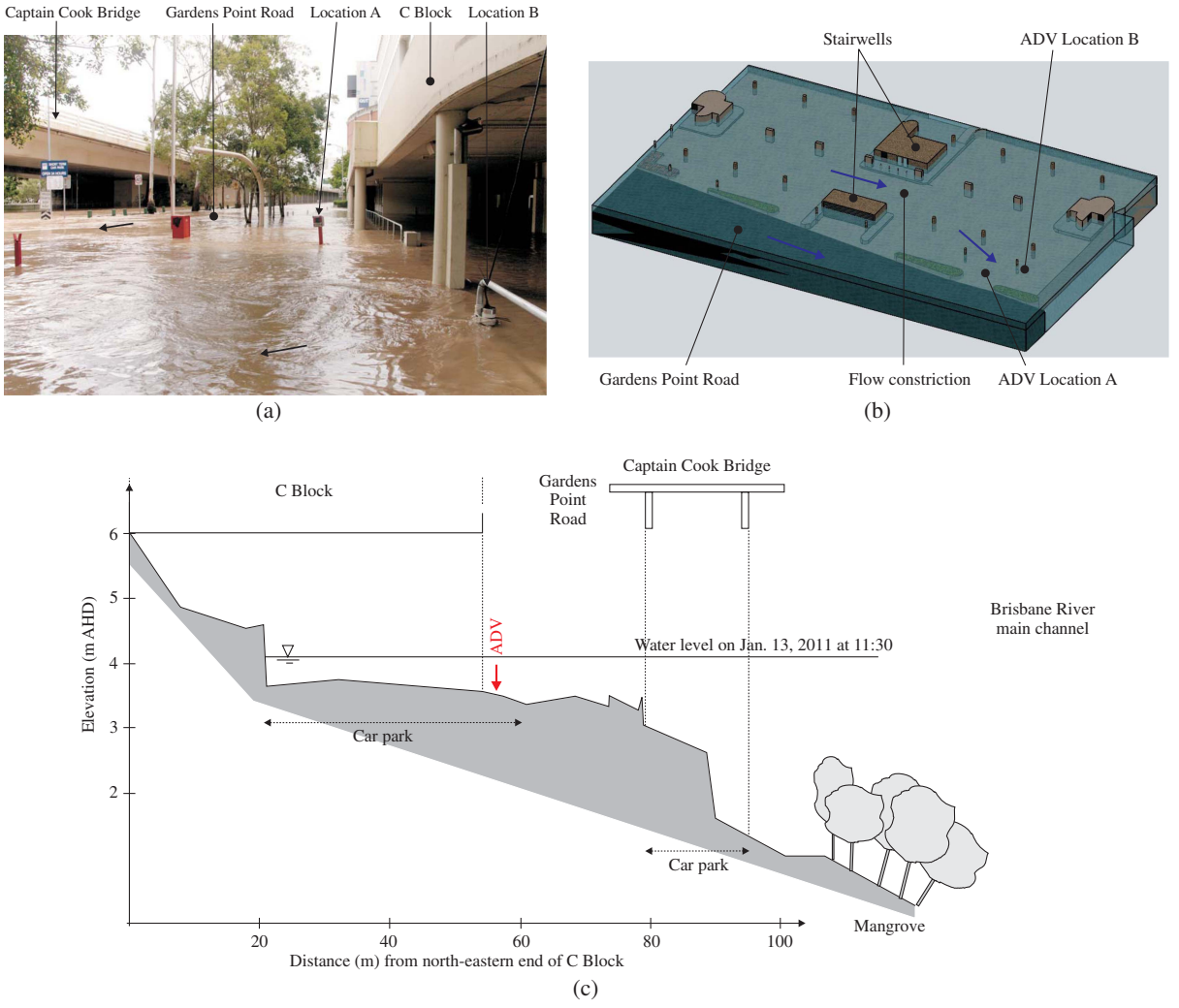

Fig. 2. Investigation site during flood: (a) flooded Gardens Points Road and submerged ADV unit on January 13, 2011, at 11:40 a.m.—arrows indicate primary flow directions; (b) C Bock submerged car park—arrows indicate primary flow directions—note constriction induced by stairwells; (c) surveyed cross section of left flood plain of Brisbane River at Gardens Point looking downstream (southeast)—arrow marks ADV location

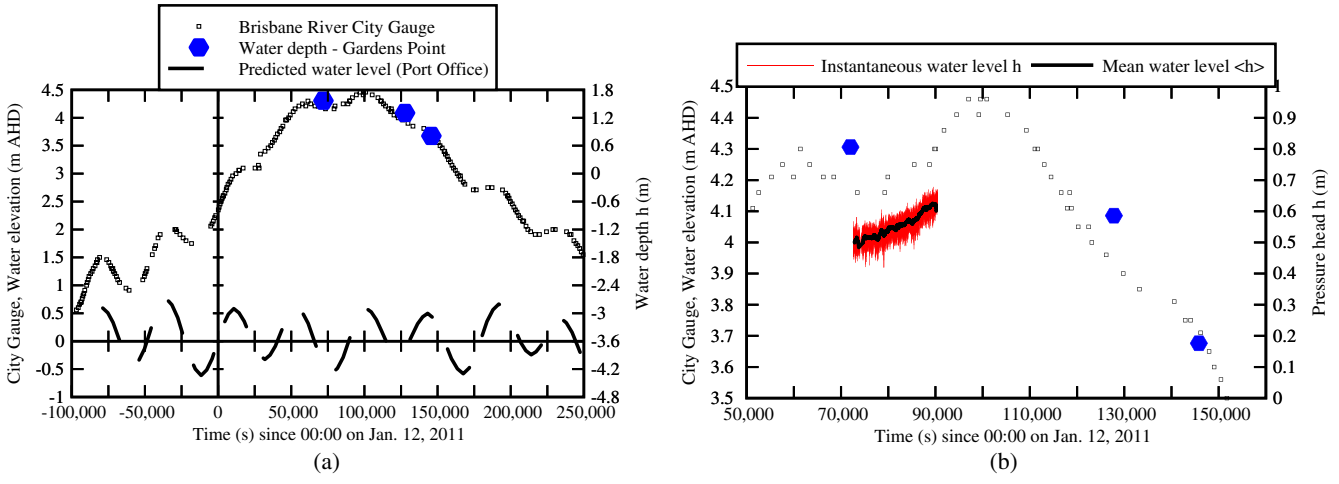

Fig. 3. Water level observations at the City Gauge (Port Office) and at Gardens Point Road: (a) Brisbane City Gauge data; predicted water elevations at Port Office and water depth observations at Gardens Point Road [reported in m Australian height datum (AHD)]; (b) instantaneous pressure head h measured above ADV pressure sensor—comparison with City Gauge data and water surface observations at Gardens Point (m AHD)

Table 1. Turbulent Velocity Measurements at Gardens Point Road During 2011 Brisbane River Flood

Data set	ADV location	Sampling rate, Hz	Velocity range, m/s	Start time	Duration	z^d, m	Flow direction[c]
1	A[a]	50	2.5	Jan. 12, 2011, at 20:40:08	4 h 26 min 40 s	0.350	160.8°
2	B[b]	50	1.0	Jan. 13, 2011, at 12:08:55	3 h 48 min 38 s	0.083	172.2°
3	B	50	1.0	Jan. 13, 2011, at 17:34:40	1 h 5 min 35 s	0.083	172.2°

[a]ADV unit mounted horizontally on boom gate support.
[b]ADV unit mounted vertically on a hand rail.
[c]Mean longitudinal flow direction at sampling location relative to the geographic North.
[d]ADV sampling volume elevation above invert.

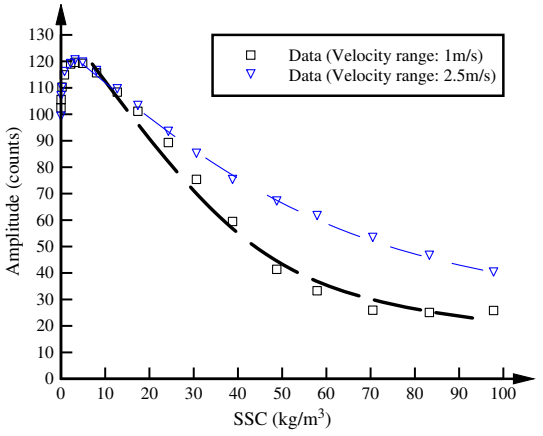

Fig. 4. Relationship between ADV signal amplitude and suspended sediment concentration for both ADV velocity settings

observations indicated that the free-surface flow in Gardens Point Road was subcritical on January 12–13, 2011. During the flood, the authors went into the C Block car park and Gardens Point Road to install the ADV system and later to relocate the unit. They observed some slow fluctuations of water level and felt some water surges with periods of about one minute. These slow fluctuations were associated with changes in water elevations of up to 0.1 to 0.2 m. On the night of January 13, the flood waters receded, leaving a 2–10-cm thick layer of soft mud.

The water depths and corresponding elevations were manually recorded on three occasions (Fig. 3, filled hexagons). The manual water depth records were 0.89 m, 0.67 m, and 0.26 m at $t = 72{,}000$ s, 127,800 s and 145,800 s, respectively. Further the pressure head above the ADV pressure sensor was recorded continuously during the first data series. The observations are reported in [Fig. 3(b)] together with the Brisbane River levels recorded at the City Gauge located 1.55 km downstream. Both the manual observations and pressure head fluctuations showed some trends that were close to the Brisbane River water level record at the City Gauge [Fig. 3(b)].

The pressure sensor readings highlighted large fluctuations of the water level around its mean trend [black thick line, Fig. 3(b)]. The measurements of water level h, longitudinal velocity V_x, and velocity flux $q = V_x h$ showed low-frequency oscillations with periods of approximately 50–100 s close to the visual observations. A spectral analysis of the data was performed. Although not shown, the lower frequency limit of the $-5/3$ slope inertial range was typically in the range of 0.5–2 Hz. Fig. 5 shows some frequency analyses of water level and velocity fluctuations during Series 1. The data sets were truncated at 0.5 Hz for clarity. The results highlighted a peak in power spectrum density (PSD) functions for periods approximately 50–100 s (approximately 60 s for Series 1 in Fig. 5) together with higher energy density levels around the characteristic peak(s). For the water level, velocity flux, velocity components, SSC, and suspended sediment flux ($q_s = V_x$SSC), the dominant slow fluctuation periods are summarized in Table 2. The results highlighted the presence of slow fluctuations with characteristic periods between 50 and 100 s for all data series in terms of water depth, velocity flux, and velocity components (Table 2). The dominant period increased with decreasing water depths. Some simple hydraulic calculations showed that it was close to the first mode of natural sloshing resonance linked with the C Block building length ($L = 70.2$ m) (Brown et al. 2011).

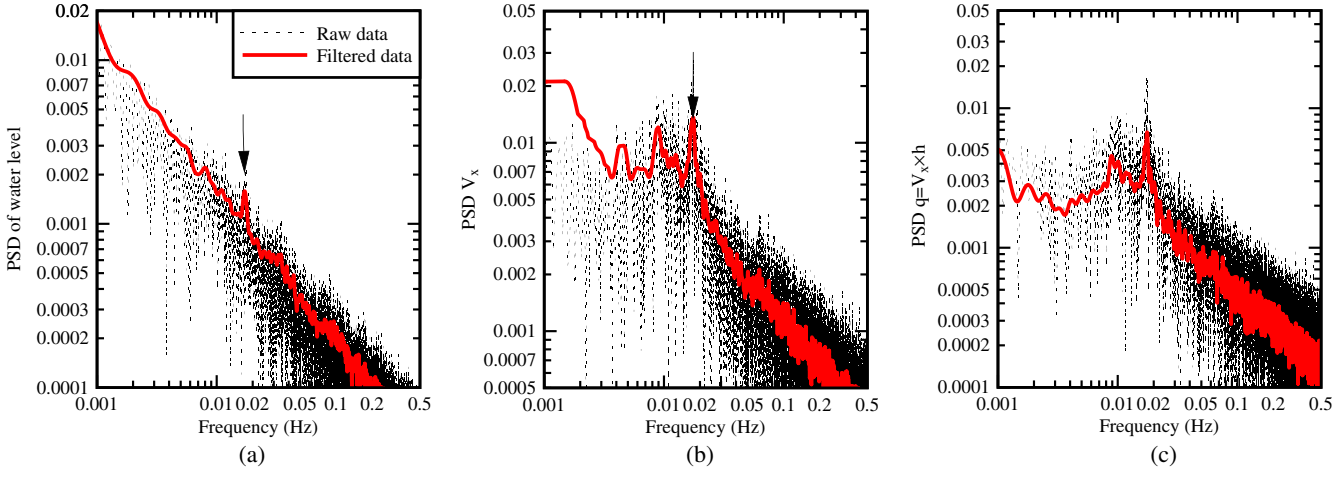

Fig. 5. Energy density spectra of water levels h, longitudinal velocity V_x, and velocity flux $q = V_x h$ during data Series 1: (a) energy density spectrum of water levels h; (b) energy density spectrum of longitudinal velocity V_x; (c) energy density spectrum of velocity flux $q = V_x h$

Table 2. Dominant Period(s) of Slow Fluctuations During Field Study in Inundated Gardens Point Road January 12–13, 2011

	Period (s)						
Data set	h	$q = h \times V_x$	V_x	V_y	V_z	SSC	$q_s = \text{SSC} \times V_x$
1	58	57	57	56	57	56	57
2	—	—	88	92	89	—	73 and 101
3	—	—	101	105	59 and 101	61	134

Discussion

At the sampling location, the flow motion was subcritical throughout the study. It is believed however, that the flow in the car park (C Block Level 1) was affected by choking in the constriction induced by two stairwells located upstream [Fig. 2(b)]. The gap between stairwells was 10 m compared to the C Block car park width of 33.6 m. Based on the observed water depth and mean longitudinal velocity data, basic hydraulic calculations show that the constricted flow could reach transcritical flow conditions between the stairwells. For a given specific energy and discharge, choking may occur when the channel constriction is too narrow, and additional specific energy is required to maintain the flow rate (Henderson 1966; Montes 1998). Energy considerations show that the total head loss in the stairwell constriction could be as large as 0.05–0.15 m during the flood flow.

When the flow in the stairwell constriction reached transcritical conditions, choking would take place, and additional energy would be required to maintain the flow rate, inducing additional head losses. The energy losses in the constriction could become substantially larger than the rate of energy loss of the main flow in Gardens Point Road, and the inundation flow would redirect around the stairwells to achieve a minimum energy path. The pattern would be responsible for some flow oscillation in the surroundings of the stairwells with a period close to the natural sloshing period of the building car park. In summary, it is believed that the excitation source of the observed slow fluctuations was some choking in the flow constriction between stairwells [Fig. 2(b)] and associated energy losses.

Flow Parameterization

As discussed in the preceding paragraph, slow-frequency fluctuations in both water elevations and velocity components were observed, and the velocity field exhibited a fluctuating behavior with periods between 50 and 100 s (Table 2). A triple decomposition of the instantaneous velocity data was performed. The technique was previously applied to periodic turbulent flows and riverine flows with large coherent structures (Hussain and Reynolds 1972; Fox et al. 2005; Yossef and de Vriend 2011).

In the present study, the instantaneous velocity time-series may be represented as a superposition of three components:

$$V = < V > + [V] + v \quad (1)$$

where V = instantaneous velocity; $< V >$ = mean velocity contribution; $[V]$ = slow fluctuating component of the velocity; and v corresponds to the turbulent motion. Herein $< V >$ is the low-pass filtered data with a cut-off frequency of 0.002 Hz ($1/500$ s^{-1}). The slow fluctuating component $[V]$ is the band-passed signal with the upper and lower cut-off frequencies set at 0.33 and 0.002 Hz ($1/3$ and $1/500$ s^{-1}, respectively). The turbulent component v is the high-pass filtered data with a cut-off frequency of 0.33 Hz ($1/3$ s^{-1}). Thus, v is zero on average, and v' is the standard deviation of the turbulent velocity component. A sensitivity analysis indicated that the low-pass filtered velocity $< V >$ was little affected by a cut-off frequency below 0.002–0.005 Hz, whereas the fast fluctuating turbulent component v and its standard deviation v' were nearly independent of an upper cut-off frequency greater than 0.1–0.3 Hz.

All the statistical properties of turbulent velocity components were calculated over a 500 s interval (25,000 data samples). The same triple decomposition treatment was applied to the water depth, velocity flux, and suspended sediment flux data. Lastly, the relative ADV sensor depth z/d was $z/d = 0.39$, 0.12, and 0.32 at $t = 72{,}000$ s, 127,800 s, and 145,800 s, respectively.

Mean Flow Properties

The water level data presented a mean trend that was close to the Brisbane River record at the City Gauge [Fig. 3(b)]. The present data provided, however, a greater level of detail because of the high-temporal resolution. The water level fluctuations were significant. On average during Series 1, the average deviation of instantaneous water level from the mean level was $(h - < h >)' = 0.10$ m. The large fluctuations were predominantly caused by relatively long-period oscillations with periods greater than 3 s. The standard deviation of the turbulent fluctuations (i.e., high-pass filtered data with 0.33 Hz cut-off) was significantly smaller: $h' = 0.003$ m, on average, for Series 1.

The velocity flux $q = V_x h$ corresponded to a longitudinal volume discharge per unit width defined in terms of the longitudinal velocity measured 0.35 m above the invert and the water level h recorded above the ADV pressure sensor. The field data showed large fluctuations of velocity flux around an almost constant trend. For data Set 1, $< q > = 0.25$ m^2/s, on average, with a deviation from mean flux $(q - < q >)' = 0.10$ m^2/s. For comparison, the standard deviation of turbulent flux fluctuations was significantly smaller: $q' = 0.018$ m^2/s, on average. The relatively large, slow fluctuations in velocity flux were consistent with the personal observations by the investigators when they were standing in the floodwater.

The time-variations of velocity components are presented in Fig. 6. Herein, V_x is the longitudinal velocity positive downstream with its direction defined in Table 1 (eighth column); V_y is the horizontal transverse velocity component; and V_z is the vertical velocity positive upwards. Each graph includes the instantaneous data V, the mean value $< V >$, and the standard deviation v' of the turbulent fluctuations. The data showed a slow decrease in longitudinal velocity magnitude during Series 1 (Location A) while the water level was gently increasing. The trend was unexpected but might be linked with some local geometry effects. During the receding flood (Series 2, Location B), the velocity magnitude decreased with increasing time and declining water level. It was quantitatively comparable to the velocity magnitude in Series 1 despite the lower flood stage. Series 3 (Location B) was conducted in very shallow waters, with local water depth ranging from 0.26 m down to 0.10 m when the ADV receivers came out of the water. The velocity magnitude was then very small: $< V_x > \approx 0.002$ m/s, on average, for Series 3.

The transverse velocity data fluctuated around zero [Fig. 6(b)]. The fluctuations were smaller than the fluctuations in the longitudinal and vertical velocity components. On average, the standard deviation of transverse velocity fluctuations about the mean was 0.4 times the standard deviation of the longitudinal

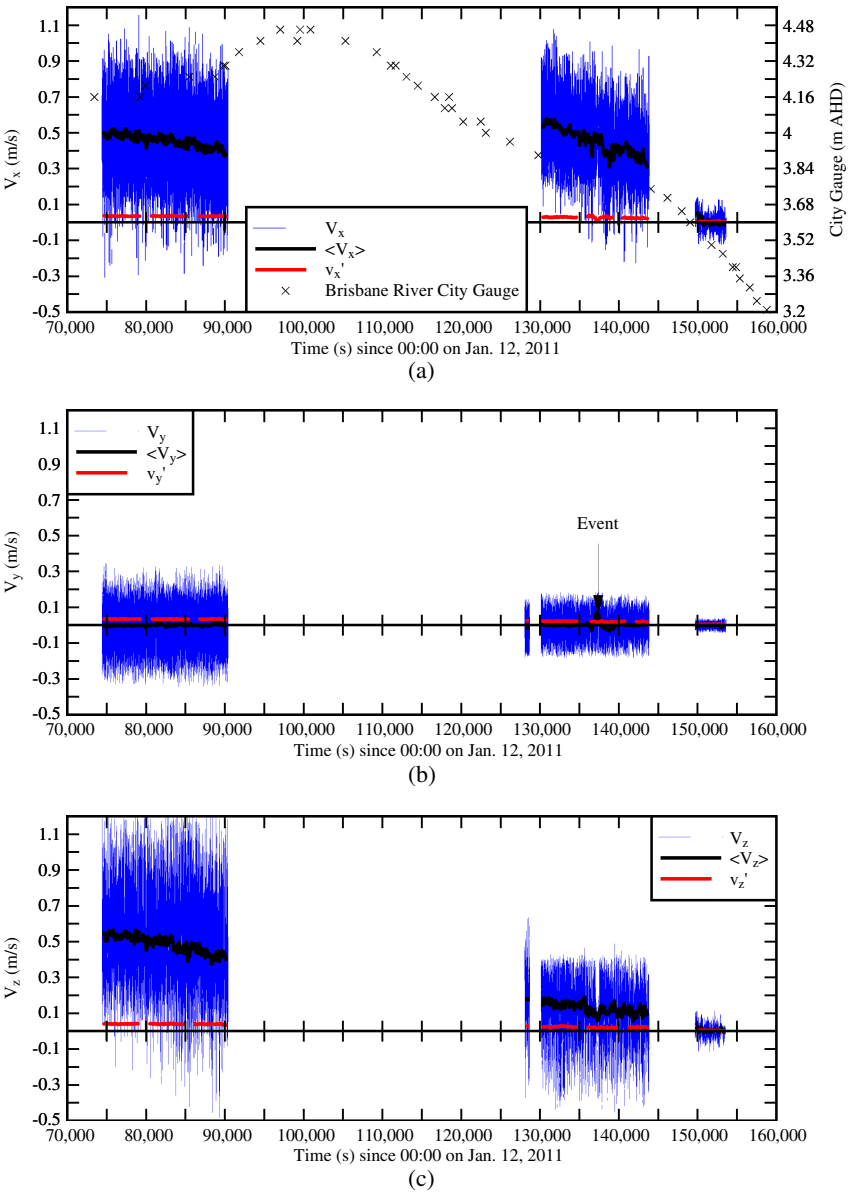

Fig. 6. Time variations of velocity components (instantaneous velocity V, mean velocity $< V >$, and standard deviation v' of turbulent fluctuation component); comparison with observed water elevations: (a) longitudinal velocity component V_x; (b) transverse velocity component V_y; (c) vertical velocity component V_z

velocity fluctuations about the mean: i.e., $(V_y - < V_y >)'/(V_x - < V_x >)' \approx 0.4$. The lesser transverse velocity fluctuations seemed to be a feature of the flood flow motion because the same trend was observed at both locations with two different ADV settings and mountings.

The vertical velocity data were typically nonzero and positive, in particular at Location A. For Series 1, the ADV unit was positioned on a pylon above a small traffic island, resulting in a flow geometry comparable to a forward-facing step. It was thought that the island kerb induced a significant modification of the streamline pattern, possibly with formation of a recirculation bubble redirecting upwards the streamlines. The exact flow pattern was complicated by the skewed flow direction with the island kerb and by the presence of surrounding obstacles, including an upstream structural column.

The velocity data indicated some unusual event during Series 2 approximately $t = 136{,}000$–$140{,}000$ s [Figs. 6(a and b)]. During this period, the mean flow direction shifted by up to 12° to the left when looking downstream [Fig. 7(a)]. The relative transverse turbulent intensity v_y'/v_x' increased sharply, as seen in Fig. 7(b), as a combination of higher values in terms of v_y' and slightly lower values in terms of v_x' during the event. The same event was associated with a sharp increase in suspended sediment flux (see the following section). The exact causes of this unusual flow pattern were unknown, but its impact on the flow in Gardens Point Road was significant and clearly recorded.

Velocity Fluctuations

The velocity data indicated some large fluctuations around the mean values (Fig. 6). These included the slow fluctuating component and the turbulent motion. An assessment of the contribution of the slow fluctuations to the total turbulence intensity was made by applying the preceding decomposition to the original velocity signal. In the power spectrum density function data [e.g., Fig. 5(b)], the turbulence of the low-frequency side of the spectrum described the slow fluctuations. The results showed that the contribution of

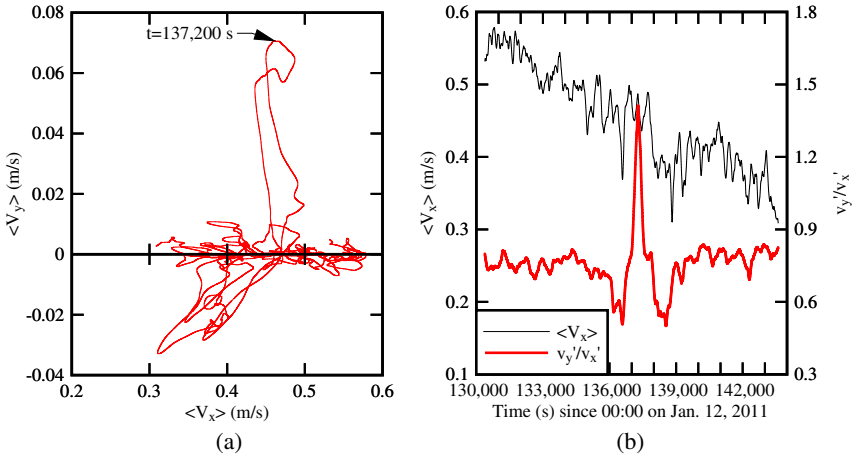

Fig. 7. Longitudinal and transverse velocity components during data Set 2: (a) horizontal velocity direction; (b) longitudinal velocity component and dimensionless ratio v_y'/v_x'

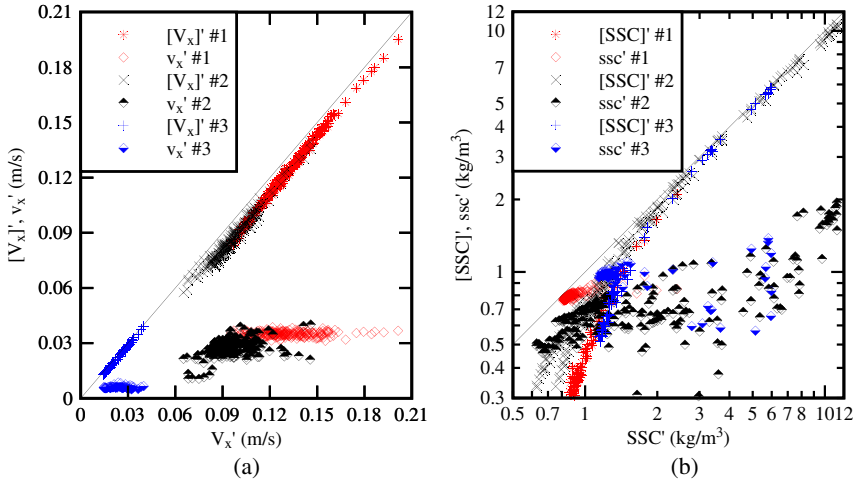

Fig. 8. Comparison of standard deviation of measured data (V_x', SSC′) to slow-fluctuating and small-scale turbulent intensities ($[V_x]'$, $[\mathrm{SSC}]'$, v_x', ssc′) (standard deviations calculated every 60 s): (a) longitudinal velocity component V_x; (b) suspended sediment concentration SSC (note logarithmic scales of axes)

small-scale turbulence fluctuations was not significant, and the slow-fluctuation turbulence intensity was nearly equal to the total [Fig. 8(a)]. Henceforth the total turbulence intensity may be used as an indication of the combined effect of large-scale turbulence and sloshing.

The longitudinal turbulent intensity $v_x'/ < V_x >$ was, on average, 5–6% for Series 1 and 2. Such a result was close to laboratory measurements in open channels although possibly slightly larger (Nezu and Nakagawa 1993; Xie 1998). The transverse and vertical relative turbulence intensities v_y'/v_x' and v_z'/v_x' showed some difference between Locations A and B. On average for Series 1 and 2, v_y'/v_x' was equal to 0.96 and 0.75 at $z = 0.35$ and 0.083 m, respectively, and v_z'/v_x' equalled 1.14 and 0.83 at $z = 0.35$ and 0.083 m, respectively. At $z = 0.35$ m, the results suggested that the turbulence was approximately isotropic: $v_x' \approx v_y' \approx v_z'$. At $z = 0.083$ m, the data indicated some anisotropy, and the overall results tended to ratios v_y'/v_x' and v_z'/v_x', close to those observed in laboratory studies with straight prismatic rectangular channels (Nezu and Nakagawa 1993; Nezu 2005; Koch and Chanson 2009).

Although the same data trend was observed for all velocity components [Fig. 8(a) showing V_x data only], a different result was observed in terms of SSC. Through most data sets, the contribution of small-scale SSC fluctuations was significant and larger than the contribution of slow fluctuations when the SSC fluctuations were less than 1.5 kg/m^3 (i.e., ssc′/SSC′ ≈ 0.72), on average for all the data. For larger SSC fluctuations (i.e., SSC′ > 1.5 kg/m^3), the slow-fluctuation turbulent term was nearly equal to the total fluctuations [Fig. 8(b)]. The findings are summarized in Table 3, showing the median values of the turbulence intensity ratios $[V]'/V'$ and v'/V' for all three velocity components and the results in terms of the suspended sediment concentration SSC and suspended sediment flux $q_s = V_x\mathrm{SSC}$ data.

Suspended Sediment Flux

The time-variations of longitudinal suspended sediment flux $q_s = V_x\mathrm{SSC}$ are presented in Fig. 9 using the high concentration limb of the appropriate calibration curve shown in Fig. 4. Herein, q_s represents the sediment flux per unit area. The suspended sediment concentrations were calculated from the measured acoustic backscatter amplitude, which was measured simultaneously with the longitudinal velocity V_x in the same sampling volume located 5 cm away from the ADV emitter. Fig. 9 includes the instantaneous data, the mean value $< q_s >$, and the standard deviation q_s' of the turbulent fluctuation component. The Brisbane City Gauge data are shown for comparison.

Table 3. Median Relative Contribution of Slow Fluctuations and Turbulent Motion on Total Turbulence Intensity at Gardens Point Road During Brisbane River Flood January 12–13, 2011

	z	$[V_x]'/V_x'$	v_x'/V_x'	$[V_y]'/V_y'$	v_y'/V_y'	$[V_z]'/V_z'$	v_z'/V_z'	$[\mathrm{SSC}]'/\mathrm{SSC}'$	$\mathrm{ssc}'/\mathrm{SSC}'$	$[q_s]'/(q_s)$	$q_s'/(q_s)'$
Data set	m	Median	Median	Median	Median	Median	Median	Median	Median	Median	Median
1	0.350	0.94	0.37	0.69	0.58	0.95	0.23	0.31	0.93	0.88	0.43
2	0.083	0.90	0.29	0.50	0.73	0.94	0.24	0.83	0.48	0.89	0.32
3	0.083	0.93	0.29	0.47	0.79	0.95	0.20	0.62	0.76	0.94	0.28

Note: Median over the data set duration; standard deviations calculated over 500 s.

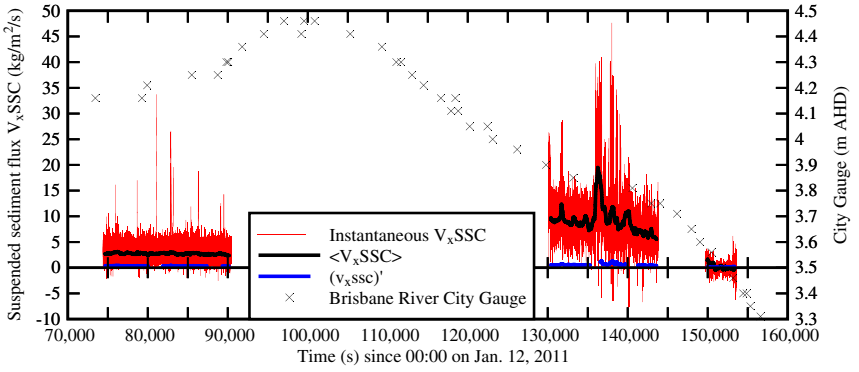

Fig. 9. Time variations of longitudinal suspended sediment flux $q_s = V_x\mathrm{SSC}$ [instantaneous suspended sediment flux, mean suspended sediment flux $< V_x\mathrm{SSC} >$, and standard deviation $(v_x\mathrm{ssc})'$ of turbulent fluctuation component]; comparison with Brisbane River City Gauge data (m AHD)

The longitudinal suspended sediment flux data q_s showed some substantial flux values, which would be consistent with the murky colour of the Brisbane River during the flood. The data highlighted a major increase in sediment flux approximately $t = 136{,}263$ s (Fig. 9). It was believed to be linked with the high values of both SSC and velocity during a major flow episode (see preceding sections). During Series 3, the data indicated some low sediment flux despite some large suspended sediment concentrations highlighted in Fig. 7. Series 3 corresponded to a period likely associated with suspended sediment deposition on the invert.

A statistical analysis suggested that most fluctuations in SSC were relatively rapid with periods less than 3 s. The results implied some differences in time scales between turbulent velocity and SSC fluctuations. The finding might suggest that the velocity fluctuations were linked with local effects and features of the urban environment, whereas the suspended sediment concentration and flux were predominantly affected by the sediment wash load.

Series 3 took place in very shallow waters (less than 0.26 m). The turbulent velocity data showed a flow pattern markedly different from the other data series (Fig. 6). The very slow flow motion suggested that the flow in the car park was disconnected from the primary river channel. The disconnection might have been caused by the concrete blocks and traffic islands between the car park and Gardens Point and between Gardens Point Road and the river bank. An alternative might be the stoppage of the flow into the C Block building car park at the northwestern end of the building.

Conclusions

During the January 2011 flood of the Brisbane River, field measurements were conducted in an inundated urban environment on the river left bank. The turbulent velocity data were collected at a relatively high frequency (50 Hz) using acoustic Doppler velocimetry in Gardens Point Road. The ADV signal amplitude was calibrated to give the suspended sediment concentration, thus providing the simultaneous measurements of three velocity components and suspended sediment flux in the same sampling volume with the same temporal resolution.

The field deployment showed some unusual features of flood flow in an urban environment. Namely, the water elevations and velocities fluctuated with distinctive periods between 50 and 100 s. These slow fluctuations were linked with some local topographic effects; that is, some local choke induced by a constriction between stairwell cases located upstream of the sampling location. The high-energy loss associated with choking would cause a flow redirection around the stairwells and some slow oscillations with a period close to the natural sloshing period of the building car park length. The instantaneous velocity data were analyzed using a triple decomposition. The same decomposition analysis was applied to the water depth, velocity flux, and suspended sediment flux data. The velocity fluctuation data showed a large energy component in the slow fluctuation range, although the turbulent motion components were much smaller: $v'/(V- < V >)' \sim 0.1$. On the other hand, the high-frequency turbulent properties were comparable to turbulent characteristics observed in turbulent boundary layers and prismatic open channel flow configurations. The suspended sediment data highlighted some significant longitudinal flux. Both velocity and suspended sediment flux data showed a major event during Series 2, which remains unexplained.

Lastly, the third data set was collected in very shallow waters, and it is suggested that the flow was disconnected from the main river channel. The turbulent properties were most likely affected by the interactions between suspended sediment deposition and flow turbulence.

This study showed that the triple decomposition approach originally developed for period flows may well be suited to complicated flood flows in an urban environment. Present results suggested that the high-frequency turbulence characteristics were

similar to turbulence properties in canonical turbulent flows, and that the contribution of slow fluctuations was significant in terms of the overall turbulent kinetic energy.

Acknowledgments

The authors thank all people who participated in the field study, as well as those who assisted with the preparation and data analysis; without them, the study would not have been possible. The authors acknowledge some helpful discussions with Dr. Frédérique Larrarte, Dr. Mark Trevethan, and Professor Laurent David. Lastly, the authors thank their respective families for their support during the difficult period of the flood in Brisbane.

Notation

The following symbols are used in this paper:

d = water depth (m);
d_{50} = median grain size (m) defined as the size for which 50% by weight of the material is finer;
h = instantaneous pressure head (m), or water level, measured above the ADV pressure sensor;
q = instantaneous longitudinal velocity flux (m^2/s): $q = V_x h$;
q_s = instantaneous longitudinal suspended sediment flux ($kg/s/m^2$): $q_s = V_x SSC$;
SSC = instantaneous suspended sediment concentration (kg/m^3);
SSC′ = standard deviation of suspended sediment concentration (kg/m^3);
ssc = turbulent suspended sediment concentration fluctuation (kg/m^3);
t = time (s);
V = instantaneous velocity (m/s): $V = < V > + [V] + v$;
V' = standard deviation of the measured velocity (m/s);
V_x = instantaneous longitudinal velocity component (m/s);
V_x' = standard deviation of the longitudinal velocity component (m/s);
V_y = instantaneous transverse velocity component (m/s);
V_z = instantaneous vertical velocity component (m/s);
$<V>$ = mean velocity (m/s) calculated as low-pass filtered data with a cut-off frequency of 0.002 Hz ($1/500\ s^{-1}$);
[V] = slow fluctuating velocity (m/s) calculated as the band-passed signal with the upper and lower cut-off frequencies set at 0.33 Hz and 0.002 Hz ($1/3\ s^{-1}$ and $1/500\ s^{-1}$, respectively);
$[V]'$ = standard deviation of the slow fluctuating velocity component (m/s);
v = turbulent velocity fluctuation (m/s): $v = V - < V > - [V]$; v is the high-pass filtered data with a cut-off frequency of 0.33 Hz ($1/3\ s^{-1}$);
v' = standard deviation of the turbulent velocity fluctuation (m/s) calculated over 500 s;
v_x' = standard deviation of the longitudinal turbulent velocity fluctuation (m/s) calculated over 500 s;
v_y' = standard deviation of the transverse turbulent velocity fluctuation (m/s) calculated over 500 s; and
v_z' = standard deviation of the vertical turbulent velocity fluctuation (m/s) calculated over 500 s.

Subscripts

x = longitudinal direction positive downstream;
y = transverse direction positive towards the left; and
z = vertical direction positive upwards.

References

Asai, Y., Ishigaki, T., Baba, Y., and Toda, K. (2010). "Safety analysis of evacuation routes considering elderly persons during underground flooding." *J. Hydrosci. Hydraul. Eng.*, 28(2), 15–21.

Bates, P. D., Horritt, M. S., Aronica, G., and Beve, K. (2004). "Bayesian updating of flood inundation likelihoods conditioned on flood extent data." *Hydrol. Processes*, 18(17), 3347–3370.

Brown, R., Chanson, H., McIntosh, D., and Madhani, J. (2011). "Turbulent velocity and suspended sediment concentration measurements in an urban environment of the Brisbane River Flood Plain at Gardens Point on 12–13 January 2011." *Hydraulic Model Rep. No. CH83/11*, School of Civil Engineering, The Univ. of Queensland, Brisbane, Australia.

Chanson, H. (2011). "The 2010–2011 floods in Queensland (Australia): Observations, first comments and personal experience." *Journal La Houille Blanche*, 1, 5–11.

Chanson, H., Reungoat, D., Simon, B., and Lubin, P. (2011). "High-frequency turbulence and suspended sediment concentration measurements in the Garonne River tidal bore." *Estuarine Coastal Shelf Sci.*, 95(2–3), 298–306.

Fox, J. F., Papanicolaou, A. N., and Kjos, L. (2005). "Eddy taxonomy methodology around submerged barb obstacle within a fixed rough bed." *J. Eng. Mech.*, 131(10), 1082–1101.

Goring, D. G., and Nikora, V. I. (2002). "Despiking acoustic doppler velocimeter data." *J. Hydaul. Eng.*, 128(1), 117–126.

Ha, H. K., Hsu, W. Y., Maa, J. P. Y., Shao, Y. Y., and Holland, C. W. (2009). "Using ADV backscatter strength for measuring suspended cohesive sediment concentration." *Cont. Shelf Res.*, 29(10), 1310–1316.

Henderson, F. M. (1966). *Open channel flow*, MacMillan, New York.

Hussain, A. K. M. F., and Reynolds, W. C. (1972). "The mechanics of on organized wave in turbulent shear flow. Part 2: Experimental results." *J. Fluid Mech.*, 54, Part 2, 241–261.

Institution of Engineers, Australia. (1974). "January 1974 floods, Moreton Region." *Proc., Symp.*, Cossins, F. and Heatherwick, G., eds., Institution of Engineers, Australia, Div., Brisbane QLD, Australia.

Ishigaki, T., Keiichi, T., and Kazuya, I. (2003). "Hydraulic model tests of 12550 inundation in urban area with underground space." *Proc., 30th IAHR Biennial Congress*, Thessaloniki, Greece, J. Ganoulis and P. Prinos, eds., Vol. B, 487–493.

Koch, C., and Chanson, H. (2009). "Turbulence measurements in positive surges and bores." *J. Hydraul. Res.*, 47(1), 29–40, 10.3826/jhr.2009.2954.

McLelland, S. J., and Nicholas, A. P. (2000). "A new method for evaluating errors in high-frequency ADV measurements." *Hydrol. Processes*, 14(2), 351–366.

Montes, J. S. (1998). *Hydraulics of open channel flow*, ASCE, New York.

Nania, L., Gomez, M., and Dolz, J. (2004). "Experimental study of the dividing flow in steep street crossings." *J. Hydraul. Res.*, 42(4), 406–412.

Nezu, I. (2005). "Open-channel flow turbulence and its research prospect in the 21st century." *J. Hydraul. Eng.*, 131(4), 229–246.

Nezu, I., and Nakagawa, H. (1993). "Turbulence in open-channel flows." *IAHR Monograph*, Int. Association for Hydro-Environment Engineering and Research (IAHR) Fluid Mechanics Section, Balkema, Rotterdam, Netherlands.

Solo-Gabriele, H. M., and Perkins, F. E. (1997). "Streamflow and suspended sediment transport in an urban environment." *J. Hydraul. Eng.*, 123(9), 807–811.

Thieken, A. H., Muller, M., Kreibich, H., and Merz, B. (2005). "Flood damage and influencing factors: New insights from the August 2002 flood in Germany." *Water Res. Resour.*, 41(12), 1–16, 10.1029/2005WR004177.

Velickovic, M., Soares-Frazao, S., and Zech, Y. (2011). "Porosity model of flow through an idealised urban district. Influence of city alignment and of transient flow character." *Proc., 34th IAHR World Congress*, E. Valentine, C. Apelt, J. Ball, H. Chanson, R. Cox, R. Ettema, G. Kuczera, M. Lambert, B. Melville, and J. Sargison, eds., Engineers Australia Publication, Barton ACT, Australia, 3823–3830.

Wahl, T. L. (2003). "Discussion of 'Despiking acoustic doppler velocimeter data' by Derek G. Goring and Vladimir I. Nikora." *J. Hydraul. Eng.*, 129(6), 484–487.

Werner, M. G. F., Hunter, N. M., and Bates, P. D. (2005). "Identifiability of distributed floodplain roughness values in flood extent estimation." *J. Hydrol.*, 314(1–4), 139–157.

Xie, Q. (1998). "Turbulent flows in non-uniform open channels: Experimental measurements and numerical modelling." Ph.D. thesis, Dept. of Civil Eng., Univ. of Queensland, Australia.

Yossef, M. F. M., and de Vriend, H. J. (2011). "Flow details near River Groynes: Experimental investigation." *J. Hydraul. Eng.*, 137(5), 504–516.